BIOCHEMISTRY
including biophysical chemistry & molecular biology

Article

pubs.acs.org/biochemistry

Another Role for CO with Nitrogenase? CO Stimulates Hydrogen Evolution Catalyzed by Variant *Azotobacter vinelandii* Mo-Nitrogenases

Karl Fisher,[†] Nathan D. Hare,[‡] and William E. Newton*

Department of Biochemistry, Virginia Polytechnic Institute and State University, Blacksburg, Virginia 24061, United States

Supporting Information

ABSTRACT: A likely entry/exit path for nitrogenase substrates, products, and/or protons involves residues $\alpha277^{Arg}$, $\alpha192^{Ser}$, and $\alpha356^{Gly}$, all of which are highly conserved among MoFe proteins from different organisms. The $\alpha192^{Ser}$ and $\alpha277^{Arg}$ residues form part of a hydrogen-bonded network that also involves $\alpha195^{His}$, which interacts with a FeMo cofactor-based sulfide. The terminal amino groups of $\alpha277^{Arg}$ are also hydrogen-bonded directly to $\alpha281^{Tyr}$, which resides at the surface of the MoFe protein. Individual amino acid substitutions placed at position $\alpha277$ or $\alpha192$ resulted in a variety of effects on the catalytic and/or spectroscopic properties of the resulting variant MoFe protein. Of particular interest was the effect of CO on H_2 evolution catalyzed by three MoFe protein variants, $\alpha277^{Cys}$, $\alpha192^{Asp}$, and $\alpha192^{Glu}$. All three variants exhibited CO stimulation of H_2 evolution under high-electron flux conditions but not under low-electron flux conditions. This observation is best explained by these variants being redox-compromised but only at the most reduced redox states of the MoFe protein. Normally, these states are accessed and operational only under high-electron flux conditions, and the effect of added CO is to prevent access to these most reduced redox states, resulting in a normal rate of catalysis. Furthermore, via correlation of the effect of pH changes on H_2 evolution activity for both the wild type and the $\alpha277^{Cys}$ MoFe protein variant under argon, with or without 10% CO present, likely pathways for the delivery of a proton to the FeMo cofactor were identified.

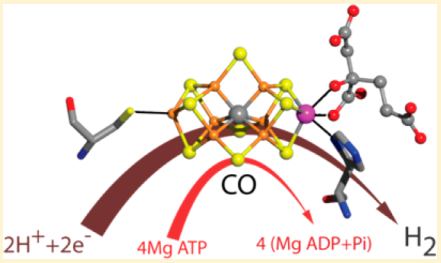

With sodium dithionite as the *in vitro* reductant, the *Azotobacter vinelandii* Mo-nitrogenase undergoes a cycle of MgATP-dependent dissociation and re-association of its two-component proteins during catalysis.[1] One component, the Fe protein, serves as the electron donor to the MoFe protein.[2] However, *in vivo*, the preferred electron donor to the Fe protein is flavodoxin hydroquinone, and its use may circumvent the need for dissociation of the two-component protein Mo-nitrogenase complex.[1,3] The MoFe protein is a 230 kDa $\alpha_2\beta_2$ heterotetramer with two copies each of two different types of prosthetic groups. Each $\alpha\beta$ dimer contains one P cluster (Fe_8S_7) located at the $\alpha\beta$ subunit interface and one FeMo cofactor (Fe_7S_9CMo-homocitrate, also called the M-center) bound within the α-subunit.[4−7] The FeMo cofactor provides the substrate- and inhibitor-binding sites.[8−10]

In addition to the reduction of N_2 to NH_3, Mo-nitrogenase catalyzes the reduction of a number of other small-molecule substrates, acetylene to ethylene and protons to H_2 being the most often utilized.[11] Some H_2 is evolved even during the catalyzed reduction of the other substrates. To account for the variety of interactions between its various substrates and inhibitors, multiple redox levels, multiple substrate-binding sites, and multiple inhibitor-binding sites have been proposed to exist on the MoFe protein.[12−17]

Carbon monoxide (CO) was used as a very potent noncompetitive reversible inhibitor of catalysis by the Mo-nitrogenase more than 70 years ago,[18] but its mechanism of action remained unclear. Its well-researched inhibitory action is to divert all electron flow to proton reduction even in the presence of other reducible substrates. However, CO inhibits catalyzed proton reduction by wild-type Mo-nitrogenase at pH >7.5[19] and by some variant Mo-nitrogenases that either contain specific amino acid substitutions[20,21] or lack homocitrate.[22,23] Moreover, anecdotal evidence suggests that CO may increase catalytic efficiency, i.e., tighten the coupling between interprotein electron transfer and MgATP hydrolysis, and also increase (~5%) the reaction rate.

More recently, CO has been recognized as playing an additional role, that of substrate, especially for the V-nitrogenase.[24] As with Mo-nitrogenase, when 10−20% CO is added to a V-nitrogenase-catalyzed reaction, reduction of the substrate (except that of the proton) is inhibited but less effectively.[25] Furthermore, at high CO concentrations, V-nitrogenase-catalyzed proton reduction itself is significantly inhibited,[26] and a small portion of its electron flux is diverted to CO reduction to produce a variety of C_1−C_4 hydrocarbons.[24] Since this discovery, exceedingly small quantities of similar CO reduction products have been detected from wild-type Mo-nitrogenase catalysis[27] and, with slightly higher yields, from use of a variant Mo-nitrogenase.[28] A similar range of concatenated

Received: May 7, 2014
Revised: September 8, 2014
Published: September 9, 2014

hydrocarbons is produced during wild-type Mo-nitrogenase-catalyzed isocyanide reduction, quite likely by a similar mechanism.[29] Recent studies using EPR/ENDOR spectroscopies,[17,21,30] SF-FTIR spectroscopy,[31,32] or infrared-monitored photolysis[33,34] are all consistent with two (at least) CO-binding sites on the FeMo cofactor.

The local environment around the FeMo cofactor within the MoFe protein α-subunit plays a major role in catalysis. Much recent research has targeted the $\alpha 70^{Val}$ residue as a gatekeeper of an avenue through which substrates and CO access the FeMo cofactor,[35] but other highly conserved amino acid residues are also involved in either substrate/inhibitor binding or proton/electron delivery (see Figure 1). In fact, a likely

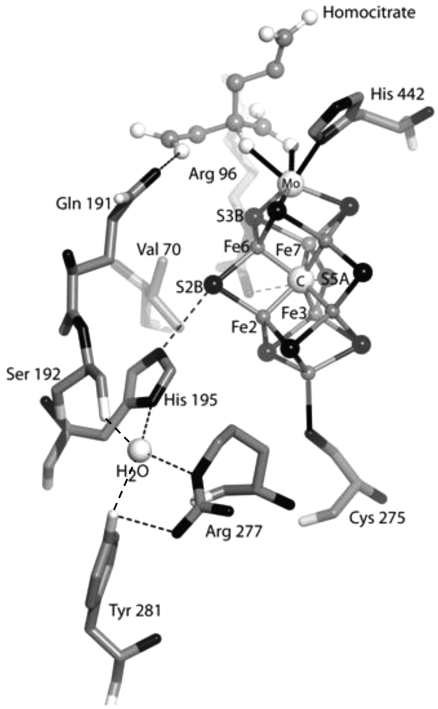

Figure 1. View of the FeMo cofactor environment of the *A. vinelandii* wild-type nitrogenase MoFe protein. The $\alpha 275^{Cys}$ and $\alpha 442^{His}$ residues that directly bind to the FeMo cofactor, along with homocitrate, $\alpha 195^{His}$, $\alpha 96^{Arg}$, and $\alpha 70^{Val}$, are shown in addition to the $\alpha 192^{Ser}$ and $\alpha 277^{Arg}$ residues that were substituted in this work. The $\alpha 356^{Gly}$ residue was omitted for the sake of clarity. Homocitrate provides two bonds to the Mo atom, which is labeled. The Fe atoms are shown as small dark gray spheres, whereas the sulfur atoms are larger and colored black. The Fe and S atoms of direct interest are labeled. The central carbide (C) is also shown. This figure was drawn from coordinates of PDB entry 1M1N.

entry/exit path for substrates, their products, and inhibitors that involves residues $\alpha 277^{Arg}$, $\alpha 192^{Ser}$, and $\alpha 356^{Gly}$ was suggested early on by analysis of the initial X-ray data acquired from the wild-type MoFe protein.[36] These three residues are highly conserved among MoFe proteins from different organisms and are located amid stretches of other highly conserved residues. The $\alpha 192^{Ser}$ and $\alpha 356^{Gly}$ residues are also conserved in the product of the *A. vinelandii nifE* biosynthetic gene, but here Lys replaces Arg at the equivalent of position $\alpha 277$, a substitution that clearly indicates that a basic charged residue is important in this position.

As shown in Figure 1, a water molecule links the ε-amino N of $\alpha 277^{Arg}$ to γ-O of $\alpha 192^{Ser}$, δ-N of $\alpha 195^{His}$ (which functions in the delivery of a proton to the FeMo cofactor[37,38]), and to the terminal hydroxyl O of $\alpha 281^{Tyr}$ (which is situated at the protein's surface and may be involved in proton capture). Substitutions at any of these positions could affect FeMo cofactor function, result in a change in the catalytic and/or spectroscopic properties of the MoFe protein, and provide insights into the functioning of the enzyme. In fact, analysis of the phenotype of several $\alpha 277$ and $\alpha 192$ mutant strains, with particular emphasis on the effect of CO on the evolution of H_2, led us to the unexpected and dramatic phenomenon of CO stimulation of H_2 evolution. Herein, we propose a rationale for explaining this phenomenon. Furthermore, we also identified the more likely pathways by which protons are delivered to form product.

MATERIALS AND METHODS

Mutant Strain Construction and Protein Purification. Site-directed mutagenesis, gene replacement, and the isolation of mutant strains carrying substitutions at position $\alpha 277$ or $\alpha 192$ were performed as described or cited previously.[39,40] Strains containing substitutions at position $\alpha 356^{Gly}$ were constructed using the Altered Sites II *in vitro* mutagenesis system from Promega (see the Supporting Information). Wild-type and mutant strains were grown on urea-supplemented Burk's media and derepressed as described previously.[14] Crude extracts were prepared by sonication, and the nitrogenase component proteins were purified as described previously,[41] except that Q-Sepharose rather than DEAE-cellulose anion-exchange chromatography was used and Sephacryl S-300 gel filtration was performed prior to and in addition to Sephacryl S-200 gel filtration. Because none of the variant MoFe proteins could be purified by crystallization, a final purification step was employed using phenyl-Sepharose hydrophobic interaction chromatography.[37] All purified nitrogenase proteins were dialyzed into 25 mM HEPES buffer (pH 7.4) before being used. Fe protein and MoFe protein specific activities were determined at each stage of purification as described previously.[37] To conduct assays at pH values other than the standard pH of 7.4, a three-component buffer system was used.[19]

Stopped-Flow Spectrophotometry. Data were collected with a Hi Tech SF-61 instrument equipped with a data acquisition and curve-fitting system (Hi Tech, Salisbury, U.K.) as described previously.[42] MoFe protein was made dithionite-free on a P-6DG gel filtration column equilibrated with 25 mM HEPES buffer (pH 7.4), with 10 mM $MgCl_2$ and 150 mM NaCl. Fe protein was oxidized, and $FldH_2$ was prepared and used as previously described.[43] All results are averages of at least five data traces, and each experiment was performed in triplicate at 23 °C.

Fe protein oxidation was monitored at 430 nm, and traces were fit to a single-exponential function. The first 30 ms of these traces was used to determine the rate of primary electron transfer. Subsequent absorbance changes [up to 1 s (Figure 5)] were collected to show the differing trends under high and low electron flux. Complex dissociation, which is rate-limiting in the wild type, was assessed as described previously.[44] The turnover rate of both the wild type and the $\alpha 277^{Cys}$ variant was also indirectly measured using the nitrogenase-dependent oxidation of $FldH_2$ as described previously (Figure 6)[43] (see the Supporting Information).

dx.doi.org/10.1021/bi500546k | *Biochemistry* 2014, 53, 6151−6160

RESULTS

Diazotrophic Growth Characteristics and Nitrogenase Crude Extract Activities. The growth phenotypes and crude extract activities of several mutants at the α277 position have been reported.[14] Here, we report the surprising result that the specific activity of evolution of H_2 from the $\alpha 277^{Cys}$ crude extract increased from 52 to 79 nmol of H_2 min^{-1} (mg of protein)$^{-1}$ when 10% CO was added to an Ar atmosphere. This ~50% increase is independent of any other reducible substrate being present and is not observed with the wild type or any other α277-substituted crude extract preparation tested. Similarly, just two (those with either Asp or Glu) of the eight mutant strains constructed at position α192 exhibited similar CO-enhanced proton reduction in crude extracts. Table S1 of the Supporting Information summarizes the diazotrophic growth behavior and crude extract specific activities for these α192 mutant strains. All extracts contain similar amounts of nitrogenase polypeptides as judged by SDS−PAGE and exhibit approximately the same levels of Fe protein activity, indicating that the substitutions have no effect on Fe protein assembly or protein expression. All the α356 mutant strains suffered complete loss of activity, which attests to the importance of $\alpha 356^{Gly}$ (and likely its glycinyl neighbor), and are no longer considered here.

Purification of the Variant $\alpha 277^{Cys}$, $\alpha 192^{Asp}$, and $\alpha 192^{Glu}$ MoFe Proteins. The variant $\alpha 277^{Cys}$, $\alpha 192^{Asp}$, and $\alpha 192^{Glu}$ MoFe proteins were purified in parallel with the wild type to minimize potential variations due to different purification protocols. SDS−PAGE revealed similar levels of purity for each protein at each stage of purification. However, although crude extracts of the $\alpha 192^{Asp}$ and $\alpha 192^{Glu}$ strains displayed proton reduction activities similar to that of the wild type, this activity decreased significantly (compared to that of the wild type) during purification, indicating that these variants are considerably less resilient than the wild type (see Table S2 of the Supporting Information). Under 100% N_2, the purified $\alpha 277^{Cys}$ MoFe protein diverts ~50% of the electron flux to H_2, whereas the $\alpha 192^{Asp}$ and $\alpha 192^{Glu}$ MoFe proteins interact very poorly with N_2 as shown by only 8 and 10% inhibition of evolution of H_2 by 100% N_2, respectively. The electrons diverted by N_2 from H_2 production with the $\alpha 192^{Glu}$ MoFe protein are used to produce ammonia; however, no ammonia production could be detected with the $\alpha 192^{Asp}$ MoFe protein.

Metal analysis of the purified MoFe proteins is reported in Table S2 of the Supporting Information. The Mo content of the purified wild-type and $\alpha 277^{Cys}$ proteins correlates well with the maximal H_2 evolution specific activity, but even in the presence of CO, both α192 variants exhibit only ~50% of the wild-type activity (see Table S2 of the Supporting Information). The catalytic and phenotypic properties of all three variants are similar to one another, but all measured kinetic parameters are higher than those of the wild type (see Table S3 of the Supporting Information).

Effect of CO on $\alpha 277^{Cys}$-Catalyzed Proton Reduction Activity as a Function of Electron Flux. Figure 2 shows the rate of H_2 evolution when the $\alpha 277^{Cys}$ MoFe protein is complemented with increasing amounts of Fe protein. N_2 reduction and C_2H_2 reduction curves are very similar in both shape and maximal obtainable specific activity (data not shown). The specific activity increases rapidly up to an ~20-fold molar excess of Fe protein over $\alpha 277^{Cys}$ MoFe protein and thereafter increases only slowly; this response is essentially

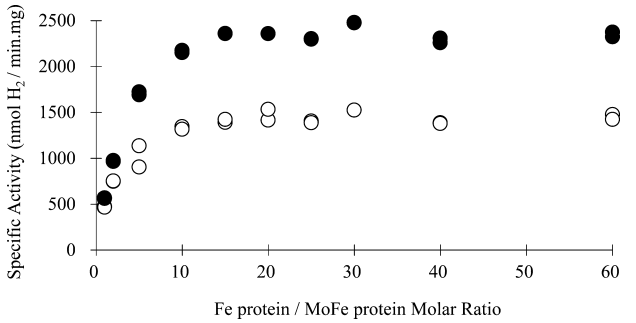

Figure 2. Effect of CO on the maximal H_2 evolution specific activity of the $\alpha 277^{Cys}$ MoFe protein when it is titrated with purified Fe protein. The 10 min assays under either 100% Ar (○) or a 10% CO/90% Ar mixture (●) contained 0.5 mg of total protein in each 1 mL assay, and the $\alpha 277^{Cys}$ MoFe protein:Fe protein molar ratio was varied accordingly.

identical to that of the wild type. Figure 2 also shows the stimulation of electron flux through the $\alpha 277^{Cys}$ MoFe protein by the addition of 10% CO. This stimulation results in an ~70% increase [from 1400 to 2400 nmol of H_2 min^{-1} (mg of MoFe protein)$^{-1}$] in activity, remains constant at a ≥5:1 Fe protein:$\alpha 277^{Cys}$ MoFe protein molar ratio, and results in a decreased ATP:2e$^-$ ratio (from 10 ± 1.0:1 to 5.4 ± 0.2:1). A similar, but even more pronounced, response to CO is exhibited by the $\alpha 192^{Asp}$ and $\alpha 192^{Glu}$ variants (see Table S2 of the Supporting Information). Decreasing the electron flux by lowering the component protein ratio below 5:1 decreases the CO enhancement of H_2 evolution, and at a ≤0.2:1 molar ratio, the rate of H_2 evolution is unaffected by adding CO. Under these low-electron flux conditions, the transfer of electrons to the product is once again more tightly coupled to the rate of MgATP hydrolysis.

Determination of Kinetic Parameters for Catalyzed C_2H_2 Reduction. Using an Fe protein:MoFe protein molar ratio of 40:1 to ensure maximal specific activity and a variety of C_2H_2 concentrations (0−20% in Ar), the determined $K_M(C_2H_2)$ values of ~2% for all three variants are significantly higher than that for the wild type (0.6%), which indicates perturbation at the C_2H_2-binding site (see Table S3 of the Supporting Information). Under standard assay conditions in the presence of 10% C_2H_2 in Ar, the $\alpha 277^{Cys}$, $\alpha 192^{Asp}$, and $\alpha 192^{Glu}$ MoFe proteins divert 74, 70, and 66% of total electron flux to C_2H_4 production, respectively. No C_2H_6 is produced. The total specific activity of the $\alpha 277^{Cys}$ MoFe protein under these conditions is ~30% less than with 10% CO, and the ATP:2e$^-$ ratio is 7.5:1 compared with 5.5:1. The CO inhibitor constant (K_i) for C_2H_2 reduction (see Table S3 of the Supporting Information), determined by measuring acetylene reduction rates as a function of C_2H_2 concentration in the presence of various CO concentrations, shows that CO is a much less potent inhibitor of reduction of C_2H_2 by the variants (K_i = 0.4−1.1%) than by the wild type (K_i = 0.05%).

H_2 Evolution under Conditions of Limiting Reductant. The low H_2 evolution rate under 100% Ar was shown not to be due to the catalyzed reduction of an unknown, but CO-sensitive, substrate by running high-electron flux assays, with a limited concentration of reductant, to exhaustion both with and without CO (Figure 3). In the absence of CO, the rate of H_2 evolution was slower but H_2 formation ultimately accounted for all reducing equivalents.

dx.doi.org/10.1021/bi500546k | Biochemistry 2014, 53, 6151−6160

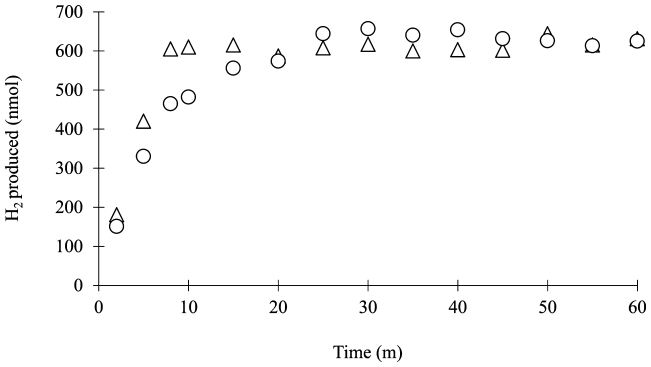

Figure 3. Time course of H_2 evolution by the $\alpha 277^{Cys}$ MoFe protein under either 100% Ar (○) or a 10% CO/90% Ar mixture (△) under conditions of limiting $Na_2S_2O_4$. Assays contained 0.25 mg of total protein at a 20:1 Fe protein:MoFe protein molar ratio. Assays were initiated every 15 s by the syringe addition of 0.1 mL of 10 mM $Na_2S_2O_4$ and terminated at the times shown by addition of 0.3 mL of 0.5 M NaEDTA (pH 7.5).

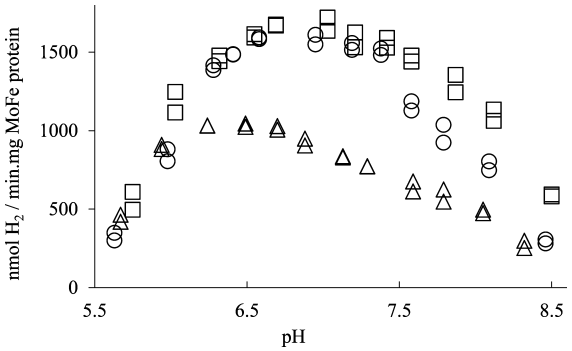

Figure 4. H_2 evolution activity vs pH profile of the $\alpha 277^{Cys}$ MoFe protein under 100% Ar and a 10% CO/90% Ar mixture. The wild-type profile under 100% Ar is included for comparison. Assays were performed as described in Materials and Methods. Assays contained 0.0415 mg of the appropriate purified MoFe protein and 0.4585 mg of purified wild-type Fe protein and were terminated after 5 min. The plots shown are (△) H_2 evolution under 100% Ar by $\alpha 277^{Cys}$ MoFe protein, (○) H_2 evolution under a 10% CO/90% Ar mixture by $\alpha 277^{Cys}$ MoFe protein, and (□) H_2 evolution under 100% Ar by wild-type MoFe protein.

Reversibility of CO Enhancement of $\alpha 277^{Cys}$ MoFe Protein H_2 Evolution. CO enhancement of H_2 evolution was shown to be reversible by measuring H_2 evolution either with or without 10% CO by terminating steady-state assays every 4 min up to 16 min. A third time course was performed in parallel initially in the presence of 10% CO, but after 8 min, these assay vials were evacuated and refilled with Ar and the subsequent H_2 production was monitored every 2 min for an additional 8 min. The removal of CO resulted in an immediate switch to the slower H_2 evolution rate observed for "Ar only" assays (see Figure S1 of the Supporting Information).

Effect of Temperature on CO-Enhanced H_2 Evolution by $\alpha 277^{Cys}$ MoFe Protein. As the assay temperature is lowered from 50 to 30 °C, the H_2 evolution activity under either a 10% CO/90% Ar mixture or 100% Ar decreases similarly such that the former remains ∼1.6 times greater than the latter. The slope of both activity versus temperature plots is 110 ± 8 activity units/°C. In the absence of CO, electron transfer remains uncoupled from ATP hydrolysis (10 ± 1:1 ATP:$2e^-$). At ≤25 °C, both slopes change, but the H_2 evolution activity under a 10% CO/90% Ar mixture (80 activity units/°C) decreases more quickly than under 100% Ar (50 activity units/°C), so that both rates converge at the lowest temperature (see Figure S2 of the Supporting Information). At ≤25 °C and under 100% Ar, electron transfer becomes increasingly coupled to MgATP hydrolysis as the temperature is decreased. At 10 °C, an ATP:$2e^-$ ratio of 5.8 ± 0.3:1 is measured, the same value that was obtained at 10 °C in the presence of 10% CO.

Specific Activity of H_2 Evolution versus pH under 100% Ar and a 90% Ar/10% CO Mixture. Figure 4 compares the specific activity versus pH profiles for the $\alpha 277^{Cys}$ MoFe protein under either 100% Ar or a 90% Ar/10% CO mixture with that of the wild type under 100% Ar. All of our pH measurements on the wild type are acid-shifted by ∼0.4 pH unit compared to those from a previous report.[19] The wild type under 100% Ar exhibits a bell-shaped curve with an optimal pH for H_2 evolution of ∼7.0 with a 50% loss of specific activity at pH ∼6.0 and ∼8.4 (the p*K* values). The $\alpha 277^{Cys}$ MoFe protein under a 90% Ar/10% CO mixture exhibits a very similar bell-shaped curve, but it is acid-shifted at higher pH values such that the p*K* is now ∼8.1. Interestingly, the wild-type profile under a 90% Ar/10% CO mixture is also acid-shifted at higher pH values such that it effectively overlays the $\alpha 277^{Cys}$ MoFe protein profile.[19,46] In contrast, under 100% Ar, the maximal specific activity of the $\alpha 277^{Cys}$ MoFe protein is decreased by ∼40% and the overall profile is dramatically acid shifted, so that the optimal pH for activity is now 6.5 and both p*K* values are acid-shifted by 0.2 pH unit.

At pH 6.0, the H_2 evolution activities of the $\alpha 277^{Cys}$ MoFe protein under 100% Ar and with 10% CO added are identical (Figure 4). We therefore monitored H_2 evolution as a function of electron flux (by varying the Fe protein:MoFe protein molar ratio) at pH 6.0. Neither the specific activity nor the ATP:$2e^-$ ratio was changed by the addition of CO over the whole tested electron flux range. Furthermore, incubating the $\alpha 277^{Cys}$ MoFe protein at pH 6.0 for 5 min before assaying it at pH 7.4 did not result in an increased rate of H_2 evolution.

Absorbance Changes Associated with Transfer of an Electron from Fe Protein to $\alpha 277^{Cys}$ MoFe Protein. The MgATP-dependent electron transfer from Fe protein to MoFe protein was monitored as an increase in absorbance at 430 nm. When the first 30 ms of this trace is fit to a single exponential, the rate of electron transfer to either wild-type or $\alpha 277^{Cys}$ MoFe protein is ∼180 s^{-1} and independent of the Fe protein concentration. At saturation, the maximal amplitude of this reaction for the $\alpha 277^{Cys}$ MoFe protein is ∼80% of that measured with the wild type; this decrease in amplitude is consistent with its lower Mo content, which reflects the fact that there are fewer active sites available to the Fe protein. There is no change in either the rate of primary electron transfer from Fe protein or the amplitude of the reaction when 10% CO is added.

We extended this pre-steady-state study to include absorbance changes that occur up to 1 s after mixing to monitor contributions from the more reduced states of the MoFe (Figure 5). Using low-electron flux conditions (1:1 Fe protein:MoFe protein molar ratio), absorbance changes with the variant MoFe proteins under an AR atmosphere are identical to those with the wild type (Figure 5A). However, at high flux (8:1 Fe protein:MoFe protein molar ratio), the absorbance increase that starts at ∼200 ms with the wild type is

dx.doi.org/10.1021/bi500546k | *Biochemistry* 2014, 53, 6151−6160

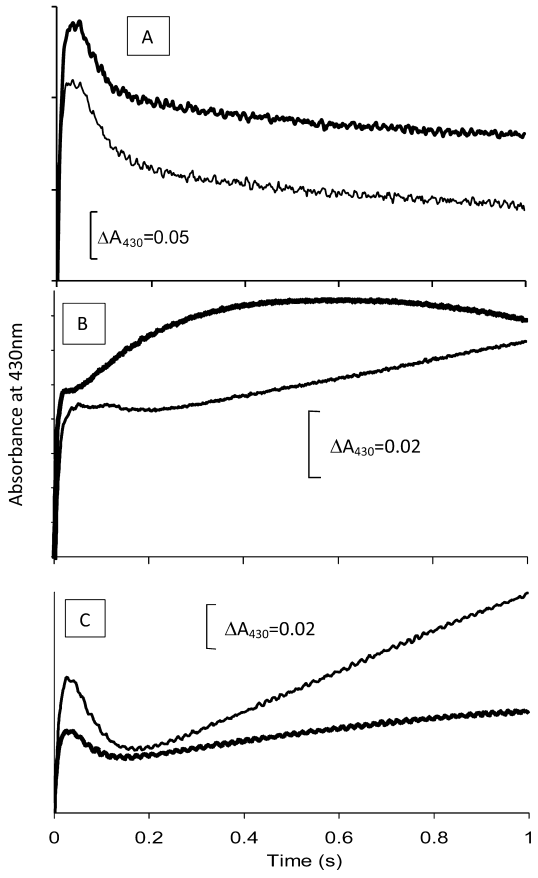

Figure 5. Stopped-flow spectrophotometry traces of absorbance changes associated with the intra-MoFe protein responses that occur after primary electron transfer from Fe protein to MoFe protein as a function of electron flux under 100% Ar. In all three panels (A–C), the wild-type data are shown as the thin line and the $\alpha 277^{Cys}$ MoFe protein data as the bold line. The traces have been arbitrarily displaced with respect to one another on the absorbance (y) axis to highlight their dependence on electron flux. All reactants were in 25 mM HEPES buffer (pH 7.4). Syringe 1 contained 18 mM MgATP, 10 mM $Na_2S_2O_4$, 9 mM creatine phosphate, and 60 μg mL^{-1} creatine phosphokinase; syringe 2 contained only nitrogenase proteins. (A) Low-electron flux conditions. After being mixed, the reaction mixture contained 10 μM Fe protein and 10 μM MoFe protein. (B) High-electron flux conditions. After being mixed, the reaction mixture contained 80 μM Fe protein and 10 μM MoFe protein. (C) High-electron flux conditions with added $FldH_2$. After being mixed, the reaction mixture contained 80 μM Fe protein, 10 μM MoFe protein, and 90 μM $FldH_2$.

not observed with the $\alpha 277^{Cys}$ MoFe protein. Instead, an oxidation starting at ~70 ms occurs (Figure 5B). The presence of either CO or C_2H_2 has no effect on this 70 ms oxidation event, but either gas significantly decreases the level of wild-type 200 ms oxidation as previously reported.[47] When a 1:1 mixture of the E_0 and E_1H redox states (see ref 2 for an explanation of this nomenclature) of the $\alpha 277^{Cys}$ MoFe protein[45] is mixed with an 8-fold excess of Fe protein in the presence of excess MgATP and dithionite, a significant increase in the magnitude of the 70 ms oxidation is observed (data not shown).

Conditions of high electron flux were employed to investigate the electron transfer reaction at pH 6.0. The rate of primary electron transfer decreased to ~20 s^{-1} with both wild-type and $\alpha 277^{Cys}$ MoFe proteins. The 70 ms oxidation of the $\alpha 277^{Cys}$ MoFe protein is no longer observable, and its longer time absorbance changes are essentially identical to those observed with the wild-type MoFe protein.

When $FldH_2$ is added to a high-electron flux sample, the 70 ms oxidation from the $\alpha 277^{Cys}$ MoFe protein is no longer present and the absorbance changes are now similar to those observed for the wild-type MoFe protein (Figure 5C). Addition of $FldH_2$ to a steady-state H_2 evolution assay under 100% Ar noticeably increases activity (by ~25%) and also more tightly couples electron transfer to MgATP hydrolysis.

Insight from the $FldH_2$ Oxidation Assay. The rate of complex dissociation[44] for the nitrogenase containing the $\alpha 277^{Cys}$ MoFe protein was found to be ~5 s^{-1}, the same as with the wild type where it is known to be rate-limiting. The rate was unaffected by added CO. The stopped-flow protocol[44] used for these measurements involves a series of reactions in which increasing concentrations of reduced Fe protein are shot against an "artificial" protein complex of chemically oxidized Fe protein, dithionite-free MoFe protein, and MgADP to force the complex apart and thereby measure the reduction of released Fe protein in a single turnover event. This protocol is incompatible with experiments based on varying the ratio of the component proteins, i.e., electron flux, so we turned to the $FldH_2$ oxidation assay[43] as a monitor of electrons transferred to nitrogenase during turnover under dithionite-free conditions to gain insight into the cause of the low turnover rate under high-electron flux conditions. From the linear rate of the absorbance change, the ε(580 nm),[48] and the concentration of active sites present (the [Mo]), turnover values of 5.5 and 5.6 s^{-1} under N_2 and N_2 with CO, respectively, were calculated for the wild type. However, for the $\alpha 277^{Cys}$ variant, at high electron flux without CO, the turnover rate is biphasic (Figure 6); after ~1.5 s, it

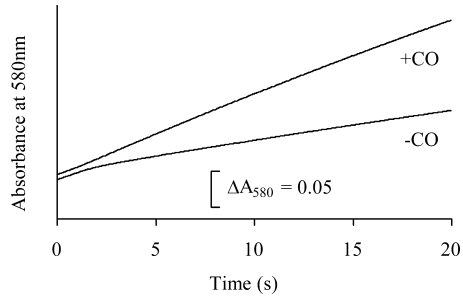

Figure 6. Measurement of the rate of $\alpha 277^{Cys}$ MoFe protein turnover by monitoring the oxidation of $FldH_2$ at 580 nm. Syringe 1 contained 1 μM MoFe protein and 8 μM Fe protein, whereas syringe 2 contained 250 μM $FldH_2$ and 9 mM ATP. Both syringes contained 25 mM HEPES buffer (pH 7.4) and 10 mM $MgCl_2$ and were dithionite-free. Where indicated, CO was added to the protein solutions by gastight syringe before they were loaded into the stopped-flow apparatus. With no CO present, the turnover rate as calculated from linear fits slows from an initial value of 4.8 s^{-1} to a value of 2.2 s^{-1} after ~1.5 s. In the presence of CO, the rate remains linear at ~6 s^{-1}.

slows from an initial value of 4.8 s^{-1} to a value of 2.2 s^{-1}. In the presence of CO at high flux, the rate remains linear at ~6 s^{-1}. The amount of $FldH_2$ oxidized during the first 1.5 s of the reaction, i.e., before the turnover rate slows, as measured from the absorbance change at 580 nm, the ε(580 nm), and the concentration of active sites present, indicates that approximately four electrons had been transferred to the $\alpha 277^{Cys}$ MoFe protein. However, if the number of electrons transferred

dx.doi.org/10.1021/bi500546k | Biochemistry 2014, 53, 6151–6160

is calculated directly from the absorbance change rate (4.8 s^{-1}) and the time elapsed (1.5 s) before the rate changes to 2.2 s^{-1}, the number is approximately seven. We have no clear explanation for this discrepancy,[49] except to point to the electron transfer problems suffered by the $\alpha 277^{Cys}$ MoFe protein and suggest that they may be contributors. Under the circumstances, we suggest that the number of electrons measured directly from $FldH_2$ oxidation, four, is likely to be the more representative.

With 20% acetylene, but no CO, present, high-flux turnover by the $\alpha 277^{Cys}$ MoFe protein occurs as a single phase but with a rate of 4.1 s^{-1}. This rate correlates well with the steady-state activity determined under 20% C_2H_2, which is intermediate between the H_2 evolution activity measured in the presence or absence of CO. At low electron flux, i.e., at a 1:1 molar protein ratio, turnover remains linear at 3 s^{-1} and is independent of CO.

The turnover rates of both $\alpha 192$ variants at high flux under N_2 are slower than with the $\alpha 277^{Cys}$ MoFe protein, in line with their lower specific activities. Both $\alpha 192$ variants are also unable to maintain the initial rate of catalysis in the absence of CO, which slows significantly after ~1.5 s from ~1.4 to ~0.5 s^{-1}. In the presence of CO, their rate of turnover again becomes a single linear phase at ~1.6 s^{-1}.

DISCUSSION

At the start of our investigation into the potential involvement of $\alpha 277^{Arg}$, $\alpha 192^{Ser}$, and $\alpha 356^{Gly}$ in substrate/inhibitor entry and/or proton/electron delivery to the FeMo cofactor, the growth phenotypes and crude extract activities of several previously reported[14] mutants with substitutions at the $\alpha 277$ position were re-assayed. In addition to confirming the previous results, an ~50% increase in the H_2 evolution activity of the $\alpha 277^{Cys}$ crude extract was found with 10% CO present. This result was completely unexpected because the $\alpha 277^{Cys}$ MoFe protein exhibits only a slight axial distortion in its resting-state $S = {}^3/_2$ EPR spectrum[21] and, when turned over under 10% CO,[30] produces the well-known axial lo-CO spectrum,[21] both of which suggested no major disturbance by the substitution in the FeMo cofactor. In contrast, the $\alpha 192^{Asp}$ and $\alpha 192^{Glu}$ variants, although with similar activity responses to added CO, are effectively Nif^- and exhibit complex EPR features. These EPR signals are essentially identical to those observed from the $\alpha 277^{His}$ MoFe protein,[14,21] which is also Nif^-. Magnitudes of both sets of signals in each of the $\alpha 192$ variants diminish in parallel under very low-flux conditions, indicating similar abilities to accept electrons. These latter signals are reminiscent of EPR signals produced during turnover by the wild type and some other variants as the more reduced states of the MoFe protein are populated.[50,51] This similarity suggests that the catalytic impediment of the $\alpha 192$ variants (and maybe the $\alpha 277^{Cys}$ MoFe protein) involves the more reduced MoFe protein redox state(s) and that added CO circumvents the effect.

Why Does Decreasing Electron Flux Abolish CO Stimulation of H_2 Evolution? All the rate constants of the Fe protein cycle[2] for these variants are unchanged from wild-type values; all are unaffected by added CO. These results, therefore, implicate reactions of the MoFe protein cycle[2] as those likely to be responsible, and this cycle is where the more reduced MoFe protein states, i.e., when multiple electrons have accumulated, are generated.

To test this hypothesis, electron flux through the nitrogenase MoFe protein was limited by (i) an unfavorable component protein molar ratio (more MoFe protein than Fe protein), (ii) changing the pH, or (iii) lowering the temperature. When the variant MoFe proteins were allowed to operate at a submaximal electron flux under any one of these adverse conditions, they operated efficiently and in a manner indistinguishable from that of the wild-type enzyme. Furthermore, when electrons were limiting, the same amount of total product was formed in the absence of CO, albeit at a decreased rate, as in its presence. Thus, the effect of CO is manifested like the effect of the adverse conditions, which is to prevent the MoFe protein from attaining its more reduced redox states. Because the activity of these MoFe protein variants is compromised under 100% Ar under high-electron flux conditions, when proton reduction from the E_3H_3 and E_4H_4 redox states should predominate,[2] it is clear that this activity impediment does not require the involvement of any other substrate, e.g., N_2, even though the variants are compromised (some totally) with respect to N_2 reduction.

How Does CO Stimulate H_2 Evolution, and Are Specific Redox States Involved? CO does not bind to the resting (E_0) state of the enzyme, but to the two-electron-reduced E_2H_2 redox state,[47] which it stabilizes sufficiently so that the more reduced N_2-binding E_3H_3 and E_4H_4 redox states are never accessed under high electron flux. All H_2 is then evolved from the E_2H_2 state.[52] This scenario is consistent with the potent noncompetitive inhibitory effect of CO on N_2 reduction. CO stimulation under high electron flux with the $\alpha 277^{Cys}$ MoFe protein is, therefore, simply explained by CO preventing the formation of the more reduced redox states (E_3H_3 and E_4H_4) and, in doing so, maintaining wild-type-like activity levels. Under low electron flux, CO has no effect because only the noncompromised E_2H_2 redox state is accessed with all H_2 evolved from this redox level.[2]

Additional insight comes from the measured rates of C_2H_2 reduction catalyzed by the variants. All of them have rates that lie between the rate of H_2 evolution under Ar alone and the rate under Ar with CO. If the E_4H_4 state alone were compromised, there would be no effect on C_2H_2 reduction because the product, C_2H_4, is evolved from the E_3H_3 state.[47] Because there is an effect on the rate, the E_3H_3 state is clearly affected. However, because the effect on the C_2H_2 reduction rate is less pronounced than that on the H_2 evolution rate under 100% Ar, the E_4H_4 state must also be compromised for H_2 evolution.

Is the Variant-Based 70 ms Oxidation Related to the Wild-Type-Based 200 ms Oxidation? An oxidation, which is observed as an absorbance increase after ~200 ms (Figure 5B) in pre-steady-state studies, occurs during wild-type catalysis under high-flux turnover conditions under either 100% N_2 or 100% Ar and has been proposed to be associated with a crucial P cluster oxidation event that signals formation of the E_4H_4 state.[52] Further, this absorbance increase is not observed when either C_2H_2 or CO is present, and this observation has been interpreted as indicating that the E_4H_4 redox state is never reached in their presence.[52] None of the three variants exhibits this 200 ms oxidation, which, on the basis of the hypothesis stated above, is consistent with them being functionally compromised with respect to the E_3H_3 and E_4H_4 redox states. Instead, a shorter time (~70 ms) oxidation occurs. Added CO has no effect on this 70 ms oxidation event, and therefore, it cannot be directly linked to the effect of CO on the low innate turnover rate. Unsurprisingly, the 70 ms oxidation is not

dx.doi.org/10.1021/bi500546k | Biochemistry 2014, 53, 6151−6160

observed when an otherwise high-flux condition reaction is monitored at pH 6.0, which, in effect, imposes low-electron flux conditions. Further, preincubation of the variant MoFe proteins at pH 6.0 does not eliminate the initially slow innate turnover rate.

Identical 70 ms oxidation events are observed with the $\alpha 277^{Thr}$, $\alpha 277^{His}$, and $\alpha 195^{Asn}$ variant MoFe proteins (unpublished data), which also have altered $S = {}^3/_2$ EPR spectra and no (or slow) diazotrophic growth capability,[9,14] but do not exhibit CO stimulation of H_2 evolution. It appears then that both $\alpha 192$ variants and the $\alpha 277^{Cys}$ variant also suffer from an intra-MoFe protein electron transfer problem, which is reflected by the 70 ms oxidation. Because the 70 ms oxidation is unaffected by added CO, this second electron transfer problem most likely involves the E_2H_2 state.

We investigated this possibility by adding $FldH_2$ to a reaction mixture under high-flux conditions. Under these conditions, the 70 ms oxidation from the variants is eliminated (Figure 5C). $FldH_2$ very rapidly reduces the oxidized Fe protein, even while it is still in a complex with the wild-type MoFe protein, but it only marginally affects the turnover rate[3] and so is unlikely to simply accelerate the slow innate turnover of the variants. However, adding $FldH_2$ increases the efficiency (a lower ATP:$2e^-$ ratio) of the reaction. This is the expected result if $FldH_2$ relieves the intramolecular electron transfer problem, such that the MoFe protein electron acceptor never becomes saturated and MgATP hydrolysis occurs only when an electron is accepted.[43] Furthermore, $FldH_2$ eliminates the small oscillation between 30 and 200 ms in the stopped-flow traces of both the wild type and variants (in Figure 5, compare panels B and C). This oscillation has been proposed to occur in response to intra-MoFe protein electron transfer reactions at the E_2H_2 redox level either between metalloclusters or to form hydrides from cluster-bound protons.[52] $FldH_2$ oxidation appears to facilitate these putative electron transfer reactions and, while doing so, relieves the cause of the 70 ms oxidation.

So, even though the 70 ms oxidation is unrelated to the 200 ms oxidation, it must arise from either the P cluster or the FeMo cofactor. The stopped-flow amplitude dependence profile indicates that the 70 ms oxidation occurs when a variant MoFe protein is being maximally serviced by the Fe protein and functioning at its full capacity. If P cluster oxidation is not observable[53] or occurs only when E_4H_4 is formed[51,52] and here E_4H_4 is never attained, then the FeMo cofactor must be oxidizing in the variants to provide electrons for H_2 evolution. If, as recently suggested,[54] the FeMo cofactor in the wild-type MoFe protein cycles between only two redox states, the $S = {}^3/_2$ EPR-active resting state and the one-electron-reduced EPR-silent state, during catalysis then any insufficiency of electrons could be supplemented by electrons released by the 70 ms oxidation to produce hydrides from bound protons.

Finally, is there a connection between the 70 ms oxidation and the change in turnover rate, which occurs after 1.5 s has elapsed? What we see is that the 70 ms oxidation is close to being over by 1 s (Figure 5B), and it is soon after [at 1.5 s (see Figure 6)] that the rate change occurs. Possibly, the source of this 70 ms oxidation and internal supply of electrons is exhausted by 1.5 s, and then only a "slower" extra MoFe protein supplier of electrons is available. With added $FldH_2$, the 70 ms oxidation is eliminated (see Figure 5C), suggesting that it may be an effective substitute for this internal electron source for at least the first 1.5 s. In this initial "quick" phase of turnover, approximately four (or so) electrons are transferred from $FldH_2$; thus, it may be that a similar number of electrons is supplied by the internal source. Because a similar "slow" phase then follows regardless of whether $FldH_2$ is present, $FldH_2$ is obviously incapable of coping with that particular catalytic impediment. Whatever the reason(s) for the "slow" turnover phase, the same process is clearly operating in all three MoFe protein variants.

Is the Delivery of a Proton to the FeMo Cofactor Affected by These Substitutions? The hydrogen-bonded network that links the $\alpha 192^{Ser}$ and $\alpha 277^{Arg}$ residues to one another and to $\alpha 195^{His}$ and the sulfide (labeled S2B in Figure 1) in the waist of the FeMo cofactor looks primed to act as a proton delivery pathway to the FeMo cofactor.[37,38] Every electron delivered to the FeMo cofactor's sulfur atoms makes them more basic and more attractive for protonation, and every such delivered electron needs an accompanying proton. A proton delivered or bound to such a sulfur atom may then be reduced to a hydrogen atom (or a hydride) that could become involved in substrate reduction.[55,56]

We investigated possible proton delivery pathways by monitoring changes in H_2 evolution activity as a function of pH. The wild-type activity versus pH profile under Ar is bell-shaped and shows that acid−base groups with p*K* values of ∼6.0 and ∼8.4 must be deprotonated and protonated, respectively, for maximal activity (Figure 4). In fact, several acid−base groups may contribute[46] to the p*K* at ∼8.4. In contrast, the $\alpha 277^{Cys}$ MoFe protein activity versus pH profile under Ar is both skewed by a dramatic acid shift and shows an ∼40% decrease in maximal H_2 evolution activity. These changes clearly indicate a direct involvement of the $\alpha 277^{Arg}$ residue in the reaction. If this substitution's only effect was to interrupt electron transfer, it might be expected to do so similarly over the complete pH range studied, but it does not. Its effect is greater at higher pH values and shifts the optimal pH value for activity. More likely, the $\alpha 277^{Arg}$ residue is a contributor to the p*K* of ∼8.4 and is involved in the delivery of protons to the FeMo cofactor.

The $\alpha 277^{Arg}$ residue has been implicated previously as a component of a hydrogen-bonded proton delivery channel that starts on the protein surface at $\alpha 281^{Tyr}$, also involves both $\alpha 192^{Ser}$ and a water molecule (164), and terminates via the $\alpha 195^{His}$ residue at the μ_2-S2B sulfur atom of the FeMo cofactor.[57] This "S2B" channel is conserved in the *A. vinelandii*, *Klebsiella pneumoniae*, and *Clostridium pasteurianum* MoFe protein structures. If this channel is a proton delivery pathway, how then does added CO negate the effects of the $\alpha 277^{Cys}$ substitution? The simplest explanation is that, under CO, the protons are delivered by a different pathway, one that does not involve the $\alpha 277$ residue. Because the profile of the wild type with CO is identical to that of the $\alpha 277^{Cys}$ variant with CO, the wild-type enzyme must also switch proton delivery channels. Consistent with this proposal, CO appears to bind at the Fe6 and/or Fe2 atoms at the "waist" of the FeMo cofactor,[15−17,33,58] both of which are μ_2-bridged by S2B, the terminus of this channel (see Figure 1). Thus, it should not be surprising that binding of CO to these Fe atoms disrupts the functioning of this "S2B channel".

But what alternative channels are available? There are two other similarly arranged μ_2-S "waist" bridges, one involving S5A between Fe7 and Fe3 and another involving S3A between Fe4 and Fe5, but neither has an obvious direct connection to the surface as required for a proton delivery channel.[57,59] However, the μ_2-S3A sulfur atom is strongly hydrogen-bonded to the

dx.doi.org/10.1021/bi500546k | *Biochemistry* 2014, 53, 6151−6160

backbone amide groups provided by α356^{Gly} and α357^{Gly}, and we found that substitution of the former leads to complete inactivation of the resulting MoFe protein variant. This result suggests a different function for the μ_2-S3A sulfur atom and its associated glycinyl residues, which may involve either stabilizing charge accumulation on the FeMo cofactor and resisting the premature loss of reducing potential as H_2 or providing flexibility for conformational changes.

A third alternative channel terminates at the μ_3-S3B atom, which bridges the Mo, Fe6, and Fe7 atoms and hydrogen bonds to a water molecule [water 679 in PDB entry 1M1N (not shown in Figure 1)].[57−59] This water molecule is also hydrogen bonded to homocitrate and, through an extensive elaborate network of water molecules, connects with the water-filled interstitial channel. This "S3B" channel is conserved in all MoFe protein structures and has also been proposed as a mode of product egress.[57] It appears to be an alternative proton delivery system that is much more efficacious than the "S5A"- and "S3A"-based systems.

Of course, depending on the requirements of the substrate present, the "S2B" channel, the "S3B" channel, or both channels could be operational in wild-type Mo-nitrogenase, with only the "S2B" channel being interrupted by the presence of CO. The "S3B" channel could be preferred for proton delivery at the E_2H_2 redox level, which is the redox limit both under CO and under lower-electron flux conditions. This suggestion is fully compatible with the wild-type activity levels observed for the α277^{Cys} variant under either CO or low-electron flux conditions, where its compromised E_3H_3 and E_4H_4 redox states would not come into play. This pathway may also be more efficient as shown by the lower ATP:2e$^-$ ratio under added CO, which may explain the anecdotal reports of CO causing tighter coupling and small rate increases.

The "S2B" channel may, therefore, become operational only when the E_3H_3 and E_4H_4 redox states are utilized, which is normally during the nitrogen fixation process. Then, the impact of substitution at residue α277 will become obvious. This suggestion is consistent with previous reports of the effectively Nif$^-$ phenotypes of, for example, the two well-studied variants, the α195^{Gln} and α277^{His} MoFe proteins.[14,37,38] Although the crystal structure of the α195^{Gln} variant is essentially the same as that of the wild type, with the glutaminyl residue maintaining the hydrogen bonding to the μ_2-S2B sulfur atom, a major difference is that the local H-bonding network has been destabilized.[60] The hydrogen bonding ability of δ-N of the imidazole ring is lost with this substitution, which results in the loss of the water molecule (water 164 in PDB entry 1M1N and water 57 in PDB entry 1QGU) from the "S2B" channel. This disruption would force reliance on the "S3B" channel and result in compromised nitrogen fixation ability. Similarly, the histidinyl substitution at the α277 position would be ideally placed to disrupt operation of the "S2B" channel. Its imidazole ring could compete with the water molecule for hydrogen bonding to either α281^{Tyr} or α195^{His} or could simply displace the water molecule; in all instances, very poor or non-N_2-fixing variants would be expected. As suggested previously for electron delivery pathways to substrate bound to the FeMo cofactor,[43] it may well be that different proton delivery systems operate for different substrates at different redox levels.

A very recent molecular dynamics approach[61] has implicated the components of the "S2B" channel as a putative substrate channel, which is gated near the protein surface by α281^{Tyr} and the nearby α383^{His} residue. These simulations also reveal significant flexibility in the positioning of residues α195^{His} and α277^{His}, which together with their free energy calculations indicate that substrate (N_2) could easily and quickly access the FeMo cofactor. As mentioned above, this channel encounters the FeMo cofactor at the 4-Fe face that binds substrate and CO.[56] Because the proton itself is a substrate, these studies and ours provide mutual support for the view that this channel is important to nitrogenase function.

In conclusion, we return to our initial question of whether we have found a new role for CO in relation to nitrogenase. The answer is no; what we actually found was CO performing its traditional inhibitory role, but under such circumstances that a different perspective was gained on how Mo-nitrogenase may manage the delivery of protons and electrons to its active sites. Under high electron flux, CO is doing what it has always done, which is to bind as an inhibitor and ensure that the E_3H_3 and E_4H_4 redox levels are never populated. The surprising result is that by binding as an inhibitor, it actually *stimulates* activity.

■ ASSOCIATED CONTENT

Ⓢ Supporting Information

Full experimental details for this article, three tables, and two figures. This material is available free of charge via the Internet at http://pubs.acs.org.

■ AUTHOR INFORMATION

Corresponding Author

*E-mail: wenewton@vt.edu. Phone: (540) 231-8431. Fax: (540) 231-9070.

Present Addresses

[†]K.F.: Manchester Institute of Biotechnology, University of Manchester, Manchester M1 7DN, U.K.

[‡]N.D.H.: Allergy Partners of Lewisburg, 2824 Old Turnpike Rd., Lewisburg, PA 17837.

Funding

This work was supported by the Virginia Agricultural Experiment Station (Project VA-135752).

Notes

The authors declare no competing financial interest.

■ ACKNOWLEDGMENTS

We thank Karin Kloos, Dennis R. Dean, and Valerie Cash (Virginia Polytechnic Institute and State University) for assistance with site-directed mutagenesis and Janet T. Rinehart and Christie H. Dapper (Virginia Polytechnic Institute and State University) for the Mo and Fe analyses.

■ ABBREVIATIONS

Mo-nitrogenase, classical molybdenum-based nitrogenase; V-nitrogenase, so-called alternative vanadium-based nitrogenase; FeMo cofactor, molybdenum- and iron-containing prosthetic group of the nitrogenase MoFe protein; Fe protein, smaller iron-containing protein component of nitrogenase (also known as component 2 or dinitrogenase reductase); MoFe protein, larger molybdenum- and iron-containing protein component of nitrogenase (also known as component 1 or dinitrogenase); P cluster, eight-iron prosthetic group of the nitrogenase MoFe protein; DEAE, diethylaminoethyl; DNase, deoxyribonuclease; EDTA, ethylenediaminetetraacetate; ENDOR, electron nuclear double resonance; EPR, electron paramagnetic resonance; $FldH_2$, flavodoxin hydroquinone; HEPES, *N*-(2-hydroxyethyl)-piperazine-*N*′-2-ethanesulfonic acid; MgADP, magnesium salt

of adenosine diphosphate; MgATP, magnesium salt of adenosine triphosphate; Nif or *nif*, nitrogen fixation; PDB, Protein Data Bank; *rif*, rifampicin; RNase, ribonuclease; SDS–PAGE, sodium dodecyl sulfate–polyacrylamide gel electrophoresis; SF-FTIR, stopped-flow Fourier transform infrared; Tris, tris(hydroxymethyl)aminomethane.

REFERENCES

(1) Hageman, R. V., and Burris, R. H. (1978) Kinetic studies on electron transfer and interaction between nitrogenase components from *Azotobacter vinelandii*. *Biochemistry 17*, 4117–4124.

(2) Lowe, D. J., and Thorneley, R. N. F. (1984) The mechanism of *Klebsiella pneumoniae* nitrogenase action. *Biochem. J. 224*, 877–909.

(3) Duyvis, M. G., Wassink, H., and Haaker, H. (1998) Nitrogenase of *Azotobacter vinelandii*: Kinetic analysis of the Fe protein redox cycle. *Biochemistry 37*, 17345–17354.

(4) Kim, J., and Rees, D. C. (1992) Crystallographic structure and functional implications of the nitrogenase molybdenum-iron protein from *Azotobacter vinelandii*. *Nature 360*, 553–560.

(5) Spatzel, T., Aksoyoglu, M., Zhang, L., Andrade, S. L. A., Schleicher, E., Weber, S., Rees, D. C., and Einsle, O. (2011) Evidence for interstitial carbon in nitrogenase FeMo cofactor. *Science 334*, 940.

(6) Lancaster, K. M., Roemelt, M., Ettenhuber, P., Hu, Y., Ribbe, M. W., Neese, F., Bergmann, U., and DeBeer, S. (2011) X-ray emission spectroscopy evidences a central carbon in the nitrogenase iron-molybdenum cofactor. *Science 334*, 974–977.

(7) Wiig, J. A., Hu, Y., Lee, C. C., and Ribbe, M. W. (2012) Radical SAM-dependent carbon insertion into the nitrogenase M-cluster. *Science 337*, 1672–1675.

(8) Shah, V. K., and Brill, W. J. (1977) Isolation of an iron-molybdenum cofactor from nitrogenase. *Proc. Natl. Acad. Sci. U.S.A. 74*, 3249–3253.

(9) Scott, D. J., May, H. D., Newton, W. E., Brigle, K. E., and Dean, D. R. (1990) Role for the nitrogenase MoFe protein α-subunit in FeMo-cofactor binding and catalysis. *Nature 343*, 188–190.

(10) Barney, B. M., Igarashi, R. Y., Dos Santos, P. C., Dean, D. R., and Seefeldt, L. C. (2004) Substrate interaction at an iron-sulfur face of the FeMo-cofactor during nitrogenase catalysis. *J. Biol. Chem. 279*, 53621–53624.

(11) Newton, W. E., and Dilworth, M. J. (2011) Assays of Nitrogenase Reaction Products. In *Nitrogen Fixation: Methods and Protocols* (Ribbe, M. W., Ed.) pp 105–127, Humana Press, New York.

(12) Hwang, J. C., Chen, C. H., and Burris, R. H. (1973) Inhibition of nitrogenase-catalyzed reductions. *Biochim. Biophys. Acta 292*, 256–270.

(13) Davis, L. C., Henzl, M. T., Burris, R. H., and Orme-Johnson, W. H. (1979) Iron-sulfur clusters in the molybdenum-iron protein component of nitrogenase. Electron paramagnetic resonance of the CO-inhibited state. *Biochemistry 18*, 4860–4869.

(14) Shen, J., Dean, D. R., and Newton, W. E. (1997) Evidence for multiple substrate-reduction sites and distinct inhibitor-binding sites from an altered *Azotobacter vinelandii* nitrogenase MoFe protein. *Biochemistry 36*, 4884–4894.

(15) Christiansen, J., Seefeldt, L. C., and Dean, D. R. (2000) Competitive substrate and inhibitor interactions at the physiologically relevant active site of nitrogenase. *J. Biol. Chem. 275*, 36104–36107.

(16) Han, J., and Newton, W. E. (2004) Differentiation of acetylene-reduction sites by stereoselective proton addition during *Azotobacter vinelandii* nitrogenase-catalyzed C_2D_2 reduction. *Biochemistry 43*, 2947–2956.

(17) Lee, H.-I., Cameron, L. M., Hales, B. J., and Hoffman, B. M. (1997) CO binding to the FeMo cofactor of CO-inhibited nitrogenase: ^{13}CO and ^{1}H Q-band ENDOR investigation. *J. Am. Chem. Soc. 119*, 10121–10126.

(18) Lind, C. J., and Wilson, P. W. (1941) Mechanism of nitrogen fixation. VIII. Carbon monoxide as an inhibitor for nitrogen fixation by red clover. *J. Am. Chem. Soc. 63*, 3511–3514.

(19) Pham, D. N., and Burgess, B. K. (1993) Nitrogenase reactivity: Effects of pH on substrate reduction and CO inhibition. *Biochemistry 32*, 13725–13731.

(20) Scott, D. J., Dean, D. R., and Newton, W. E. (1992) Nitrogenase-catalyzed ethane production and CO-sensitive hydrogen evolution from MoFe proteins having amino acid substitutions in an α-subunit FeMo cofactor-binding domain. *J. Biol. Chem. 267*, 20002–20010.

(21) Maskos, Z., Fisher, K., Sørlie, M., Newton, W. E., and Hales, B. J. (2005) Variant MoFe proteins of *Azotobacter vinelandii*: Effects of carbon monoxide on electron paramagnetic resonance spectra generated during enzyme turnover. *JBIC, J. Biol. Inorg. Chem. 10*, 394–406.

(22) McLean, P. A., and Dixon, R. A. (1981) Requirement of *nifV* gene for production of wild-type nitrogenase enzyme in *Klebsiella pneumoniae*. *Nature 292*, 655–656.

(23) Hoover, T. R., Imperial, J., Ludden, P. W., and Shah, V. K. (1989) Homocitrate is a component of the iron-molybdenum cofactor of nitrogenase. *Biochemistry 28*, 2766–2771.

(24) Lee, C. C., Hu, Y., and Ribbe, M. W. (2010) Vanadium nitrogenase reduces CO. *Science 329*, 642.

(25) Dilworth, M. J., Eady, R. R., and Eldridge, M. E. (1988) The vanadium nitrogenase of *Azotobacter vinelandii*. Reduction of acetylene and ethylene to ethane. *Biochem. J. 249*, 745–751.

(26) Lee, C. C., Hu, Y., and Ribbe, M. W. (2009) Unique features of the nitrogenase VFe protein from *Azotobacter vinelandii*. *Proc. Natl. Acad. Sci. U.S.A. 106*, 9209–9214.

(27) Hu, Y., Lee, C. C., and Ribbe, M. W. (2011) Extending the carbon chain: Hydrocarbon formation catalyzed by vanadium/molybdenum nitrogenases. *Science 333*, 753–755.

(28) Yang, Z. Y., Dean, D. R., and Seefeldt, L. C. (2011) Molydenum nitrogenase catalyzes the reduction and coupling of CO to form hydrocarbons. *J. Biol. Chem. 286*, 19417–19421.

(29) Kelly, M., Postgate, J. R., and Richards, R. L. (1967) Reduction of cyanide and isocyanide by nitrogenase of *Azotobacter chroococcum*. *Biochem. J. 102*, 1c–3c.

(30) Cameron, L. M., and Hales, B. J. (1996) Investigation of CO binding and release from Mo-nitrogenase during catalytic turnover. *J. Am. Chem. Soc. 118*, 279–280.

(31) George, S. J., Ashby, G. A., Wharton, C. W., and Thorneley, R. N. F. (1997) Time-resolved binding of carbon monoxide to nitrogenase monitored by stopped-flow infrared spectroscopy. *J. Am. Chem. Soc. 119*, 6450–6451.

(32) Yang, Z.-Y., Seefeldt, L. C., Dean, D. R., Cramer, S. P., and George, S. J. (2011) Steric control of the hi-CO MoFe nitrogenase complex revealed by stopped-flow infrared spectroscopy. *Angew. Chem., Int. Ed. 50*, 272–275.

(33) Yan, L., Dapper, C. H., George, S. J., Wang, H.-X., Mitra, D., Dong, W.-B., Newton, W. E., and Cramer, S. P. (2011) Photolysis of hi-CO nitrogenase: Observation of a plethora of distinct CO species using infrared spectroscopy. *Eur. J. Inorg. Chem. 2011*, 2064–2074.

(34) Yan, L., Pelmenschikov, V., Dapper, C. H., Scott, A. D., Newton, W. E., and Cramer, S. P. (2012) IR-monitored photolysis of CO-inhibited nitrogenase: A major EPR-silent species with coupled terminal CO ligands. *Chemistry 18*, 16349–16357.

(35) Seefeldt, L. C., Hoffman, B. M., and Dean, D. R. (2009) Mechanism of Mo-dependent nitrogenase. *Annu. Rev. Biochem. 78*, 701–722.

(36) Kim, J., and Rees, D. C. (1992) Structural models for the metal centers in the nitrogenase molybdenum-iron protein. *Science 257*, 1677–1682.

(37) Kim, C.-H., Newton, W. E., and Dean, D. R. (1995) Role of the MoFe protein α-subunit histidine-195 residue in FeMo-cofactor binding and nitrogenase catalysis. *Biochemistry 34*, 2798–2808.

(38) Fisher, K., Dilworth, M. J., and Newton, W. E. (2000) Differential effects on N_2 binding and reduction, HD formation, and azide reduction with α-195^{His}- and α-191^{Gln}-substituted MoFe proteins of *Azotobacter vinelandii* nitrogenase. *Biochemistry 39*, 15570–15577.

(39) Brigle, K. E., Setterquist, R. A., Dean, D. R., Cantwell, J. S., Weiss, M. C., and Newton, W. E. (1987) Site-directed mutagenesis of the nitrogenase MoFe protein of *Azotobacter vinelandii*. *Proc. Natl. Acad. Sci. U.S.A. 84*, 7066−7069.
(40) Jacobson, M. R., Brigle, K. E., Bennett, L. T., Setterquist, R. A., Wilson, M. S., Cash, V. L., Beynon, J., Newton, W. E., and Dean, D. R. (1989) Physical and genetic map of the major *nif* gene cluster from *Azotobacter vinelandii*. *J. Bacteriol. 171*, 1017−1027.
(41) Burgess, B. K., Jacobs, D. B., and Stiefel, E. I. (1980) Large-scale purification of high activity *Azotobacter vinelandii* nitrogenase. *Biochim. Biophys. Acta 614*, 196−209.
(42) Ashby, G. A., and Thorneley, R. N. F. (1987) Nitrogenase of *Klebsiella pneumoniae*: Kinetic studies on the Fe protein involving reduction by sodium dithionite, the binding of MgADP and a conformational change that alters the reactivity of the 4Fe-4S centre. *Biochem. J. 246*, 455−465.
(43) Peters, J. W., Fisher, K., Newton, W. E., and Dean, D. R. (1995) Involvement of the P cluster in intramolecular electron transfer within the nitrogenase MoFe protein. *J. Biol. Chem. 270*, 27007−27013.
(44) Thorneley, R. N. F., and Lowe, D. J. (1983) Nitrogenase of *Klebsiella pneumoniae*. Kinetics of the dissociation of oxidized iron protein from molybdenum-iron protein: Identification of the rate-limiting step for substrate reduction. *Biochem. J. 215*, 393−403.
(45) Fisher, K., Lowe, D. J., and Thorneley, R. N. F. (1991) *Klebsiella pneumoniae* nitrogenase. The pre-steady-state kinetics of MoFe-protein reduction and hydrogen evolution under conditions of limiting electron flux show that the rates of association with the Fe-protein and electron transfer are independent of the oxidation level of the MoFe protein. *Biochem. J. 279*, 81−85.
(46) Newton, W. E., Vichitphan, K., and Fisher, K. (2002) Substrate reduction and CO susceptibility of the ΔNifV and α-Q191K MoFe proteins of *Azotobacter vinelandii* nitrogenase. In *Nitrogen Fixation: Global Prospects* (Finan, T., O'Brian, M., Layzell, D., Vessey, K., and Newton, W. E., Eds.) p 370, CAB International, Wallingford, U.K.
(47) Lowe, D. J., Fisher, K., and Thorneley, R. N. F. (1990) *Klebsiella pneumoniae* nitrogenase. Mechanism of acetylene reduction and its inhibition by carbon monoxide. *Biochem. J. 272*, 621−625.
(48) Klugkist, J., Voorberg, J., Haaker, H., and Veeger, C. (1986) Characterization of three different flavodoxins from *Azotobacter vinelandii*. *Eur. J. Biochem. 155*, 33−40.
(49) We thank a reviewer for pointing out this discrepancy.
(50) Fisher, K., Newton, W. E., and Lowe, D. J. (2001) Electron paramagnetic resonance analysis of different *Azotobacter vinelandii* nitrogenase MoFe-protein conformations generated during enzyme turnover: Evidence for $S = {}^3/_2$ spin states from reduced MoFe-protein intermediates. *Biochemistry 40*, 3333−3339.
(51) Fisher, K., Lowe, D. J., Tavares, P., Pereira, A. S., Huynh, B. H., Edmondson, D., and Newton, W. E. (2007) Conformations generated during turnover of the *Azotobacter vinelandii* MoFe protein and their relationship to physiological function. *J. Inorg. Biochem. 101*, 1649−1656.
(52) Lowe, D. J., Fisher, K., and Thorneley, R. N. F. (1993) *Klebsiella pneumoniae* nitrogenase. Pre-steady-state absorbance changes show redox changes occur in the MoFe protein that depend on substrate and component protein ratio; a role for P-centres in reducing dinitrogen? *Biochem. J. 292*, 93−98.
(53) Danyal, K., Dean, D. R., Hoffman, B. M., and Seefeldt, L. C. (2011) Electron transfer within nitrogenase: Evidence for a deficit-spending mechanism. *Biochemistry 50*, 9255−9263.
(54) Doan, P. E., Telser, J., Barney, B. M., Igarashi, R. Y., Dean, D. R., Seefeldt, L. C., and Hoffman, B. M. (2011) ^{57}Fe ENDOR spectroscopy and "electron inventory" analysis of the nitrogenase E_4 intermediate suggest the metal-ion core of FeMo-cofactor cycles through only one redox couple. *J. Am. Chem. Soc. 133*, 17329−17340.
(55) Dance, I. (2006) Mechanistic significance of the preparatory migration of hydrogen atoms around the FeMo-co active site of nitrogenase. *Biochemistry 45*, 6328−6340.
(56) Hoffman, B. M., Lukoyanov, D., Yang, Z.-Y., Dean, D. R., and Seefeldt, L. C. (2014) Mechanism of nitrogen fixation by nitrogenase: The next stage. *Chem. Rev. 114*, 4041−4062 and references cited therein.
(57) Durrant, M. C. (2001) Controlled protonation of iron-molybdenum cofactor by nitrogenase: A structural and theoretical analysis. *Biochem. J. 355*, 569−576.
(58) Dance, I. (2011) Calculated vibrational frequencies for FeMo-co, the active site of nitrogenase, bearing hydrogen atoms and carbon monoxide. *Dalton Trans. 40*, 6480−6489.
(59) Dance, I. (2005) The hydrogen chemistry of the FeMo-co active site of nitrogenase. *J. Am. Chem. Soc. 127*, 10925−10942.
(60) Sørlie, M., Christiansen, J., Lemon, B. J., Peters, J. W., Dean, D. R., and Hales, B. J. (2001) Mechanistic Features and Structure of the Nitrogenase α-Gln^{195} MoFe Protein. *Biochemistry 40*, 1540−1549.
(61) Smith, D., Danyal, K., Raugei, S., and Seefeldt, L. C. (2014) Substrate channel in nitrogenase revealed by a molecular dynamics approach. *Biochemistry 53*, 2278−2285.